Available online at www.sciencedirect.com
ScienceDirect
Catalysis Today 129 (2007) 297–304
CATALYSIS TODAY
www.elsevier.com/locate/cattod

Partial oxidation of ethanol on Ru/Y_2O_3 and Pd/Y_2O_3 catalysts for hydrogen production

A.M. Silva [a], A.P.M.G. Barandas [a], L.O.O. Costa [a,b], L.E.P. Borges [b], L.V. Mattos [a], F.B. Noronha [a,*]

[a] *Instituto Nacional de Tecnologia – INT, Av. Venezuela 82, CEP 20081-310, Rio de Janeiro – RJ, Brazil*
[b] *Instituto Militar de Engenharia – Praça General Tibúrcio, 80, Praia Vermelha, Rio de Janeiro 22290-270, Brazil*

Available online 25 September 2007

Abstract

The partial oxidation of ethanol was investigated over Ru and Pd catalysts supported onto yttria over a wide range of temperatures (473–1073 K). The product distributions obtained over these catalytic systems were correlated with diffuse reflectance infrared spectroscopy analyses (DRIFTS). Results showed that reaction route depended strongly on the type of metal. The decomposition of ethoxy species to CH_4 and CO or oxidation to CO_2 was promoted by Pd, and the acetaldehyde desorption was predominant over Ru in the low temperature region. Furthermore, the acetate and carbonate formation prevailed over Pd, which explained the lower acetaldehyde selectivity. The presence of CH_4 and CO_2 at high temperature is assigned to the decomposition of acetate species via carbonates over Pd-based catalysts. Ru was more suitable system for H_2 production than Pd by achieving a selectivity of about 59%.

Keywords: Partial oxidation of ethanol; H_2 production; Fuel cell

1. Introduction

Hydrogen is one of the most abundant elements in the universe. However, hydrogen is not a primary source of energy and hence it needs to be manufactured. Hydrogen can be obtained from a variety of energy sources such as: (i) fossil fuels like coal, natural gas and oil; (ii) biomass (agricultural and forestry residues, industrial and municipal wastes) (iii) renewable energy sources such as solar or wind energy through water electrolysis [1–4].

Nowadays, the technology for hydrogen production is well known for large units (10,000–100,000 Nm^3/h or larger) and is based on hydrocarbon steam reforming [5,6]. The majority of hydrogen is produced in refineries to upgrade crude oil (hydrocracking and hydrotreating process), in the petrochemical industry to synthesize different chemical compounds (such as ammonia and methanol), in the oil and fat hydrogenation and in metallurgical process (as a reduction gas) [7].

But, the current hydrogen industry does not produce H_2 as an energy carrier or as a fuel for energy generation [8]. Hence, the installed H_2 production and distribution infrastructure is insufficient to support its widespread use in a hydrogen economy. In the absence of a hydrogen infrastructure in the early stages of the transition to a hydrogen economy, hydrogen needs to be produced locally at refueling stations, which faces new challenges. Distributed hydrogen production via small-scale reforming at refueling stations could be an attractive near to mid-term option for supplying hydrogen [9]. However, lower pressure and temperature are needed to make small-scale reforming competitive. Several small-scale reformer technologies are currently being developed, such as steam reforming, partial oxidation and autothermal reforming, to produce hydrogen from different feedstocks (hydrocarbons such as methane and gasoline; alcohols such as methanol and ethanol) [10].

In contrast to fossil fuels, ethanol is a renewable raw material that can be obtained from biomass and can address the issue of the greenhouse effect. Furthermore, the infrastructure needed for ethanol production and distribution is already established in countries like Brazil and USA where ethanol is currently distributed and blended with gasoline.

* Corresponding author. Fax: +55 21 2206 1051.
E-mail address: fabiobel@int.gov.br (F.B. Noronha).

0920-5861/$ – see front matter
doi:10.1016/j.cattod.2006.09.036

Hydrogen may be produced from ethanol through steam reforming [11–18], oxidative steam reforming [19–23] and partial oxidation [19,24–28]. In particular, partial oxidation systems have fast start up and response time, which make them attractive for following rapidly varying loads. Moreover, the partial oxidation (POX) reactor is more compact than a steam reformer, since it does not need the indirect addition of heat via a heat exchanger.

However, hydrogen production from ethanol presents some disadvantages such as catalytic deactivation [29] and formation of by-products [30]. The major cause of catalyst deactivation during hydrogen production from ethanol is carbon deposition [31]. Another challenge is the formation of by-products, which decreases not only the hydrogen yield but also the fuel cell performance. There are several reaction pathways that may occur during the ethanol reactions [24–26,32–34]. In fact, ethanol reactions on transition metal surfaces are a very complex system, including several reaction intermediates [35]. For example, the specific bonding configuration of the acetaldehyde compounds on transition metal surfaces (η^1(O); η^2(C, O)) is directly correlated to their thermal stability on these surfaces. Therefore, the reaction pathways and the product distribution observed on ethanol reactions on transition metal surfaces are strongly dependent on the nature of both metal and support.

There are only few studies about the effect of metal and support on the partial oxidation of ethanol [24,27,28].

Wang et al. [28] evaluated the effect of Ni/Fe ratio on the performance of Ni and Fe-based catalysts ($Ni_{90}Fe_{10}$, $Ni_{70}Fe_{30}$, $Ni_{50}Fe_{50}$, $Ni_{30}Fe_{70}$, $Ni_{10}Fe_{90}$) at 573 K and O_2/ethanol = 1.5. All catalysts presented a good performance on partial oxidation of ethanol. However, $Ni_{50}Fe_{50}$ showed the highest ethanol conversion (86.91%) and H_2 selectivity (50.66%). The good performance of Ni–Fe catalysts was related to the presence of spinel-structured (Ni, Fe) Fe_2O_4 and $FeNi_3$ alloys, which are probably the active species for partial oxidation of ethanol.

Salge et al. [27] studied the partial oxidation of ethanol over noble metals (Rh, Ru, Pd and Pt) and metal plus ceria-coated alumina foams at 973 K and C/O = 0.7. Rh–Ce was more stable than noble metals alone. Concerning H_2 selectivity, Rh–Ce presented the highest H_2 production (∼80%). Among noble metals, Pt and Pd showed the lower formation of H_2 (<50%). The by-products obtained were CH_4, C_2H_4 and acetaldehyde for all catalysts. However, Pt, Pd and Rh exhibited higher selectivity to CH_4 and C_2H_4 than Rh–Ce. The better performance of Rh–Ce was assigned to redox properties of Ce.

We studied the effect of metal nature on the performance of ceria-supported catalysts on partial oxidation of ethanol at 573 K and O_2/ethanol molar ratio of 0.5 [24]. The results revealed that the Pt/CeO_2 catalyst produced the higher initial activity (∼80%) and the product distribution is strongly affected by the nature of the metal. Acetaldehyde was practically the only product formed on Co/CeO_2 catalyst while methane was also produced on Pt/CeO_2 and Pd/CeO_2 catalysts. A reaction mechanism was proposed to explain the results based on IR and Temperature Programmed Desorption (TPD) of ethanol experiments.

In the literature, some researchers have reported that the support plays an important role on the steam reforming of ethanol [36–38]. However, there are few works dealing with the effect of support on partial oxidation of ethanol [25]. We studied the effect of the nature of the support on the performance of Pt/Al_2O_3, Pt/ZrO_2, Pt/CeO_2 and $Pt/Ce_{0.50}Zr_{0.50}O_2$ catalysts on partial oxidation of ethanol [25]. The results showed that the support plays an important role on the products distribution of the partial oxidation of ethanol. Acetic acid was the main product on Pt/Al_2O_3 catalyst whereas methane and acetaldehyde were the only products detected on Pt/ZrO_2, Pt/CeO_2 and $Pt/Ce_{0.50}Zr_{0.50}O_2$ catalysts. The product distribution obtained over these catalysts was correlated to their redox and acid properties.

The aim of this work is to study the effect of the metal nature on the performance of Y_2O_3 supported catalysts on the partial oxidation of ethanol. Yttria was chosen as a basic support. These results will be compared with our previous work involving redox and acidic support.

2. Experimental

2.1. Catalyst preparation

Y_2O_3 support was prepared by calcination of yttrium nitrate (Aldrich) at 1073 K for 1 h. The catalysts were prepared by incipient wetness impregnation of the support with an aqueous solution containing palladium and ruthenium nitrates. After impregnation, the samples were dried at 393 K and calcined under air (50 cm^3/min) at 673 K, for 2 h.

2.2. X-ray fluorescence (XRF)

The chemical composition of the samples was determined by X-ray fluorescence on a RIGAKU (RIX3100) equipment.

2.3. Brunauer Emmett and Telle (BET) surface area

The BET surface areas of the catalysts were measured using a Micromeritics ASAP 2000 analyzer by nitrogen adsorption at liquid nitrogen temperature.

2.4. Infrared spectroscopy

Diffuse reflectance infrared spectroscopy analyses (DRIFTS) were performed using a Fourier transform infrared spectrometer (Magna 560 Nicolet) coupled to a SpectraTech high temperature cell. Before the analysis, the samples were reduced with H_2 at 773 K, for 2 h. Then, they were cooled down to room temperature under helium, and a mixture containing an ethanol/O_2 molar ratio = 2 was passed through the catalysts. The spectra were collected at 298, 373, 473, 573, 673 and 773 K.

2.5. Reaction conditions

Ethanol partial oxidation was performed in a fixed-bed reactor at atmospheric pressure. In order to avoid hot spot formation and temperature gradients, catalyst samples

(160 mg) were diluted with SiC (catalyst/SiC ratio = 1:3) to form a small catalyst bed (<5 mm in height). The temperature of the catalyst bed was measured through a thermocouple inserted in a small cavity on the reactor wall. Prior to reaction, the samples were reduced under H_2 at 773 K, for 1 h. The reactants were fed to the reactor by bubbling air (30 cm^3/min) and N_2 (30 cm^3/min) through a saturator containing ethanol at 313 K, in order to obtain the desired ethanol/O_2 molar ratio (2:1). The reaction was carried out at different temperatures and W/Q = 0.16 g s cm^{-3} (W = weight of catalyst; Q = volumetric flow rate). The exit gases were analyzed using a gas chromatograph (VARIAN, CP 3800) equipped with two columns (molecular sieve and parabond Q/CP 7424—select permanent gases/CO_2) coupled in parallel with a thermal conductivity and a flame ionization detectors connected in series.

2.6. Thermogravimetric analysis

Thermogravimetric analysis of the used catalysts was carried out on a TA instruments equipment (TGA 2050). The samples were heated under air from room temperature to 1273 K at a heating rate of 5 K/min.

3. Results and discussion

3.1. Catalysts characterization of fresh catalysts

The metal loading and the BET surface area obtained for all samples are presented in Table 1. Ru/Y_2O_3 and Pd/Y_2O_3 catalysts contained 1.52 and 0.93 wt% of ruthenium and palladium, respectively. The surface area of the Y_2O_3 support, Ru/Y_2O_3 catalyst and Pd/Y_2O_3 catalyst were very low (16–24 m^2/g).

3.2. Partial oxidation of ethanol

The partial oxidation of ethanol was carried out in a wide range of temperatures (473–1073 K) on Y_2O_3 support, Ru/Y_2O_3 and Pd/Y_2O_3 catalysts. The catalytic activity was evaluated by ethanol conversion. The carbon balance was around 100% at the temperature range studied for all samples.

3.2.1. Partial oxidation of ethanol on Y_2O_3 support

Fig. 1 shows the ethanol conversion and products distribution obtained over Y_2O_3 support. The complete ethanol conversion was achieved at 773 K.

At 473 K, water and acetaldehyde were the only products obtained. The increase of reaction temperature decreased the selectivity to water. Regarding acetaldehyde production, it was observed significant amounts between 473 and 573 K. Increasing the reaction temperature strongly decreased the acetaldehyde formation. At 773 K, acetaldehyde was no longer detected.

H_2 selectivity was very low in all temperature ranges studied, reaching a maximum (~14%) at 1073 K. The increase of reaction temperature from 473 to 873 K favored the CO formation.

Concerning CH_4 formation, small amounts (~4–6%) were only observed above 773 K. In case of CO_2 production, when the temperature was increased from 473 to 673 K, the selectivity to CO_2 increased. Nevertheless, at temperatures higher than 673 K, the formation of CO_2 remained practically stable.

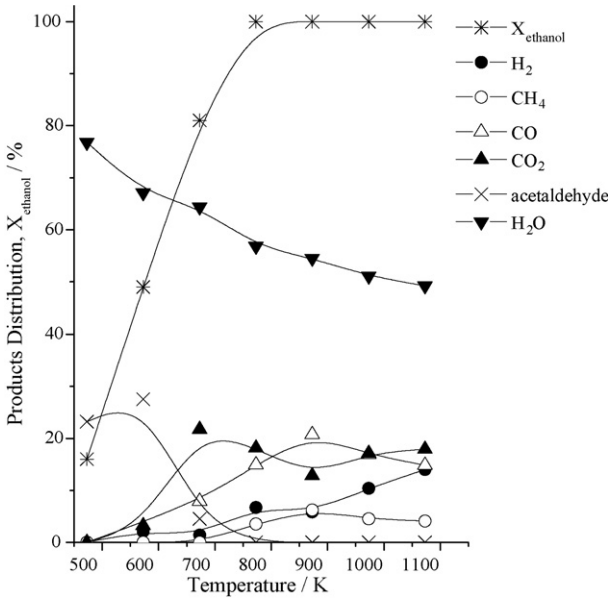

Fig. 1. Products distribution and ethanol conversion ($X_{ethanol}$) on partial oxidation of ethanol as a function of reaction temperature (473–1073 K) over Y_2O_3 support. Reaction conditions: W/Q = 0.16 g s cm^{-3}; ethanol/O_2 molar ratio = 2.

Table 1
Metal loading and BET surface areas of Y_2O_3 and supported Ru and Pd catalysts

Sample	Metal loading (wt%)	BET surface area ($m^2/g_{catalyst}$)
Y_2O_3	–	18.4
Ru/Y_2O_3	1.52	24.3
Pd/Y_2O_3	0.93	16.1

3.2.2. Partial oxidation of ethanol on Ru/Y_2O_3 and Pd/Y_2O_3 catalysts

The ethanol conversion and products distribution obtained over Ru/Y_2O_3 and Pd/Y_2O_3 catalysts are depicted in Figs. 2 and 3, respectively. Ru/Y_2O_3 and Pd/Y_2O_3 catalysts exhibited approximately similar activities over the entire temperature range. The complete ethanol conversion was achieved for both systems at 873 K.

Figs. 2 and 3 revealed that the product distribution was strongly affected by the reaction temperature and the nature of the noble metal. Basically, the main products were water and acetaldehyde at 473 K. The selectivity to H_2O was around 50% for both catalysts in the temperature range of 473–773 K. As the temperature increased the water formation was gradually suppressed. Nevertheless, on Pd/Y_2O_3 significant amounts of H_2O (around 13%) were found even at 1073 K; on Ru/Y_2O_3 this value was lower than 1%.

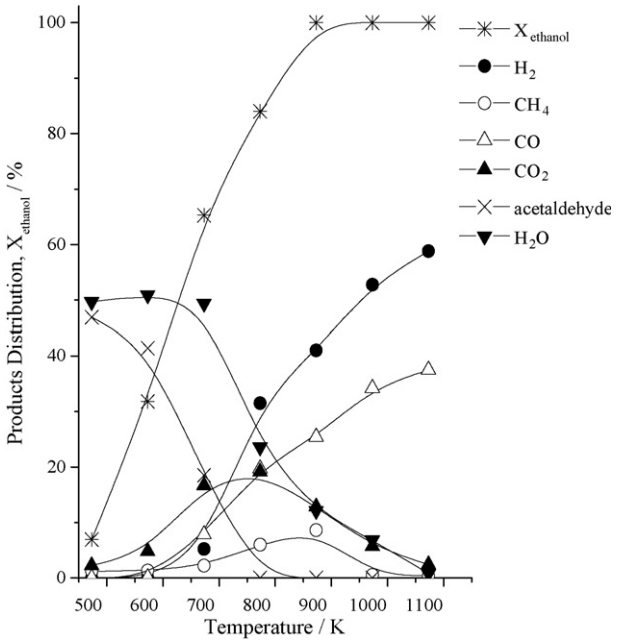

Fig. 2. Products distribution and ethanol conversion ($X_{ethanol}$) on partial oxidation of ethanol as a function of reaction temperature (473–1073 K) over Ru/Y_2O_3 catalyst. Reaction conditions: W/Q = 0.16 g s cm^{-3}; ethanol/O_2 molar ratio = 2.

Likewise, acetaldehyde formation was favored at temperatures lower than 773 K for both catalysts. However, Ru/Y_2O_3 led to higher acetaldehyde selectivity over all temperatures. Acetaldehyde was no longer detected above 773 K for both the catalysts.

H_2, CO, CO_2 and CH_4 were produced over both catalysts. In contrast with the results of Y_2O_3 support, significant amounts of H_2 were produced at temperatures higher than 673 K.

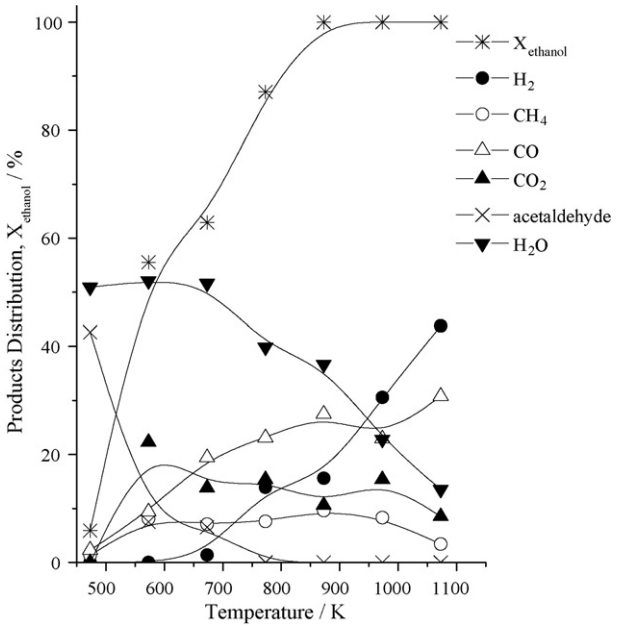

Fig. 3. Products distribution and ethanol conversion ($X_{ethanol}$) on partial oxidation of ethanol as a function of reaction temperature over Pd/Y_2O_3 catalyst. Reaction conditions: W/Q = 0.16 g s cm^{-3}; ethanol/O_2 molar ratio = 2.

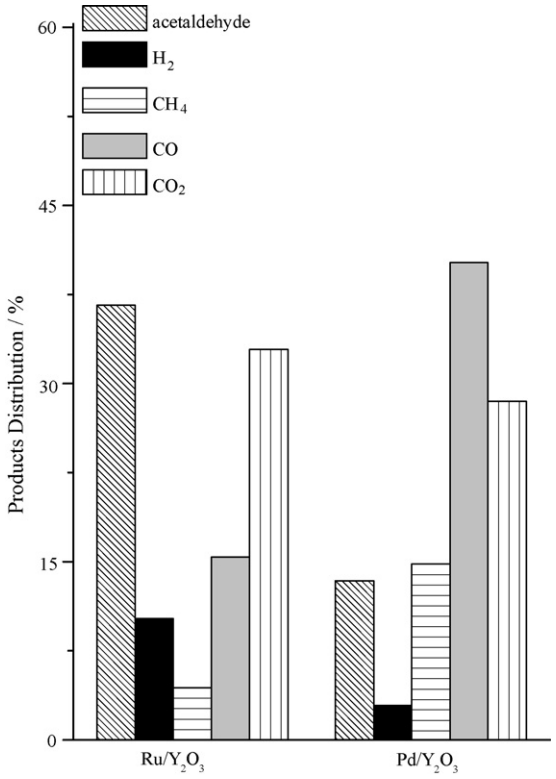

Fig. 4. Products distribution in dry basis obtained at the same conversion on partial oxidation of ethanol over Ru/Y_2O_3 and Pd/Y_2O_3 catalysts. Reaction conditions: W/Q = 0.16 g s cm^{-3}; ethanol/O_2 molar ratio = 2.

Moreover, Ru/Y_2O_3 was more selective than Pd/Y_2O_3 in the studied temperature range. The maximum H_2 selectivity (59%) was achieved on Ru/Y_2O_3 catalyst at 1073 K. H_2 production was accompanied by the CO formation, displaying a similar trend upon heating. Pd/Y_2O_3 presented higher selectivity to CO at temperatures between 473 and 773 K. Above this temperature range, Ru/Y_2O_3 was more selective than Pd/Y_2O_3 toward CO formation.

Concerning CO_2 and CH_4 formation, these products were observed at all temperatures investigated on Pd/Y_2O_3. On the other hand, Ru/Y_2O_3 exhibited a maximum in the CO_2 and CH_4 production at 773 and 873 K, respectively. Only traces of these products were detected over Ru/Y_2O_3 catalyst at 1073 K.

Fig. 4 displays the products distribution for Ru/Y_2O_3 and Pd/Y_2O_3 catalysts in dry basis at the same ethanol conversion (∼65%) which was obtained at 673 K for both catalysts. The products detected were acetaldehyde, H_2, CH_4, CO and CO_2. However, the product distributions for both the catalysts were quite different. From Fig. 4, it is clear that acetaldehyde formation was favored on Ru/Y_2O_3 reaching 37% of selectivity while this value did not exceed 13% over Pd/Y_2O_3. On the other hand, the Ru/Y_2O_3 catalyst was the most effective system for H_2 production. Significant amount of CO was found over both the catalysts. However, Pd/Y_2O_3 exhibited 40% of CO selectivity and a lower value (15%) was obtained for Ru/Y_2O_3. As a matter of fact, the H_2/CO ratio obtained for Ru catalyst was about 10 times higher than Pd catalyst. At this conversion, Pd/Y_2O_3 and Ru/Y_2O_3 showed 4 and 15% of CH_4 selectivity,

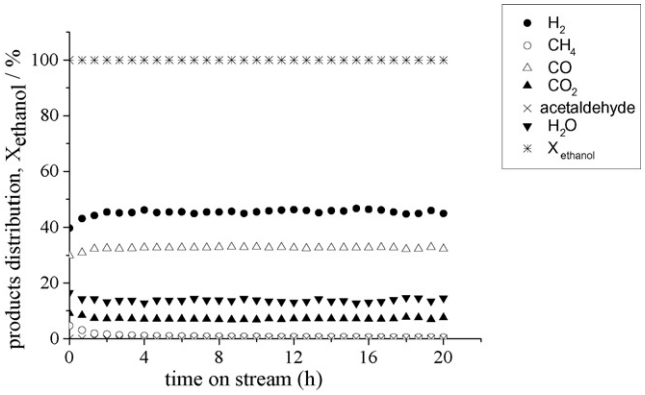

Fig. 5. Products distribution and ethanol conversion ($X_{ethanol}$) on partial oxidation of ethanol as a function of time on stream over Pd/Y_2O_3 catalyst. Reaction conditions: $W/Q = 0.16$ g s cm^{-3}; ethanol/O_2 molar ratio = 2; reaction temperature = 1073 K.

respectively. Regarding the CO_2 production similar amounts were obtained for both the catalysts.

3.2.3. Catalyst stability

The stability of the Ru/Y_2O_3 and Pd/Y_2O_3 catalysts on partial oxidation of ethanol was evaluated at 1073 K. The results obtained for Pd/Y_2O_3 catalyst are exhibited in Fig. 5. This catalyst is quite stable after 20 h time-on-stream. Moreover, the selectivities to the products also remained constant along the run. The performance of Ru/Y_2O_3 catalyst (not shown) was similar to that observed for Pd-based catalyst.

3.3. Thermogravimetric analysis

Fig. 6 shows the results obtained by thermogravimetric analysis for Pd/Y_2O_3 catalyst, after reaction at different temperatures. Two small peaks were observed at 655 and 873 K. The results obtained for Ru/Y_2O_3 catalyst were similar

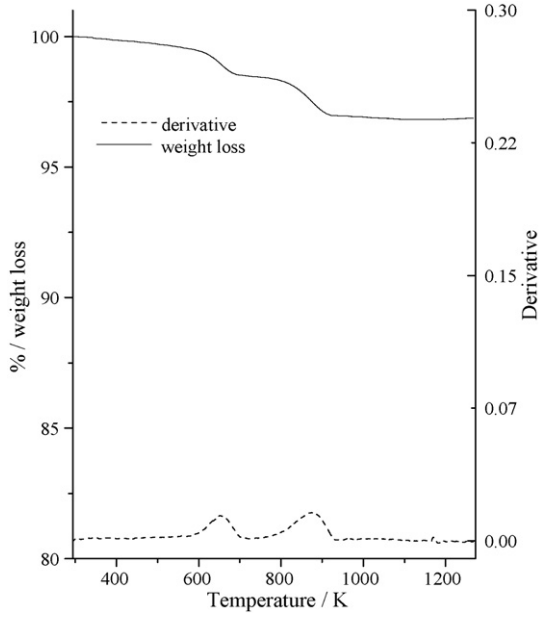

Fig. 6. Thermogravimetric analysis for Pd/Y_2O_3 catalyst, after reaction.

Table 2
Amount of carbon (mass of carbon/mass of catalyst) produced during the partial oxidation of ethanol on Ru/Y_2O_3 and Pd/Y_2O_3 catalysts

Sample	Amount of carbon ($mg_{carbon}/mg_{catalyst}$)
Ru/Y_2O_3	0.0081
Pd/Y_2O_3	0.025

to those observed for Pd-based catalyst. The amount of carbon corresponding to these peaks for Ru/Y_2O_3 and Pd/Y_2O_3 catalysts is presented in Table 2. The results show that the formation of carbon was very low on both the catalysts. These results are in agreement with those presented in Fig. 5, which confirms that there is no significant carbon deposition on catalysts surface during partial oxidation of ethanol under these reaction conditions.

3.4. Diffuse reflectance infrared spectroscopy (DRIFTS)

The results obtained on partial oxidation of ethanol suggest a strong influence of the metal nature on products distribution. Therefore, to better understand the catalytic performance and correlate them with the metal properties, the intermediates of partial oxidation of ethanol were monitored by DRIFTS analysis.

3.4.1. IR spectra of Y_2O_3 support

The IR spectra of ethanol adsorbed on Y_2O_3 support are presented in Fig. 7. The spectra obtained at room temperature showed bands at 1054, 1094 and 1379 cm^{-1} which can be attributed to ethoxy species [26,39–42]. The ethoxy species formation occurs by dissociative adsorption of ethanol. By heating to 373 K no significant changes in the spectra were

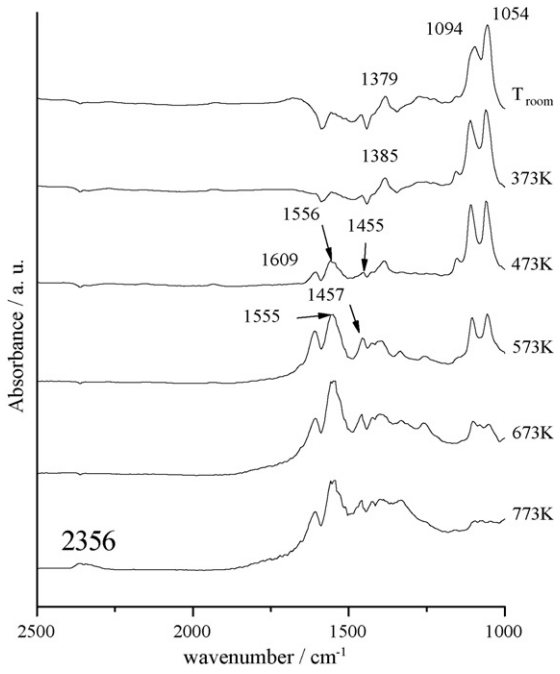

Fig. 7. Infrared spectra of the surface species formed by ethanol adsorption on Y_2O_3 support at different temperatures.

observed. At 473 K, besides those bands related to ethoxy species, vibrations were also detected at 1455 and 1556 cm^{-1}, assigned to acetate species [39–42]. The band at 1609 cm^{-1} is due to the presence of hydrogen carbonate species [43,44]. Acetate species were produced through further oxidation of ethoxy species by gas phase oxygen. These acetate species were then further oxidized to hydrogen carbonate species.

The presence of acetate species on ceria-supported catalysts after ethanol adsorption was previously reported in the literature [26,39–42]. However, it is interesting to note that on CeO_2-supported catalysts the acetate formation was detected even at room temperature [26]. This behavior was due to the redox properties of ceria. Since yttria lacks redox properties, the acetate species were only produced at higher temperatures (≥473 K) through oxidation of ethoxy species by gas phase oxygen.

The increase of acetate formation was followed by the disappearance of ethoxy species as the temperature increased. At 773 K, the bands corresponding to ethoxy species disappeared completely while the acetate species were still present. Moreover, a band in the 2300–2400 cm^{-1} region related to CO_2 was observed, which resulted from the oxidation of acetate species.

3.4.2. IR spectra of Ru/Y_2O_3 catalyst

IR spectra of Ru/Y_2O_3 catalyst are depicted in Fig. 8. According to Fig. 8, after ethanol adsorption at room temperature, vibrations associated to ethoxy species at 1049, 1087 cm^{-1} and to acetyl species at 1647 cm^{-1} were formed on Ru/Y_2O_3. The acetyl species result from the additional hydrogen atom elimination of the adsorbed acetaldehyde. This intermediate was already experimentally identified [35] and its formation corroborated by theoretical models [45].

At 373 K, the appearance of both the acetate species at 1029, 1342 1410, 1451 and 1578 cm^{-1} and the hydrogen carbonate species (shoulder at 1609 cm^{-1}) as well as the decrease of the intensity of the ethoxy species vibrations were noted on Ru/Y_2O_3. These results suggest that ethoxy species were oxidized to acetate species and then to hydrogen carbonate species. However, the oxidation of ethoxy species is not probably the only reaction occurring at this temperature. Several works have reported the appearance of CO, CH_4 and H_2 at the low temperature region during FTIR and TPD analysis of adsorbed ethanol, which was attributed to the decomposition of ethoxy species [26,40,46–48]. This result revealed that the ethoxy species were also decomposed at this temperature.

By heating to 473 K the characteristic bands of acetate and hydrogen carbonate species increased. At temperatures higher than 473 K, these bands remained practically unchanged. The bands associated to CO_2 production were only observed at 773 K. CO_2 formation was also reported in the literature and it was associated with the decomposition of carbonate species [43].

3.4.3. IR spectra of Pd/Y_2O_3 catalyst

Ethoxy species with vibrations at 1056 and 1091 cm^{-1} were also detected on Pd/Y_2O_3 spectrum after ethanol adsorption at room temperature (Fig. 9). Interestingly on Pd-based catalyst, the acetate species (1024, 1056, 1338, 1420, 1456 and 1571 cm^{-1}) and the hydrogen carbonate species (1601 cm^{-1})

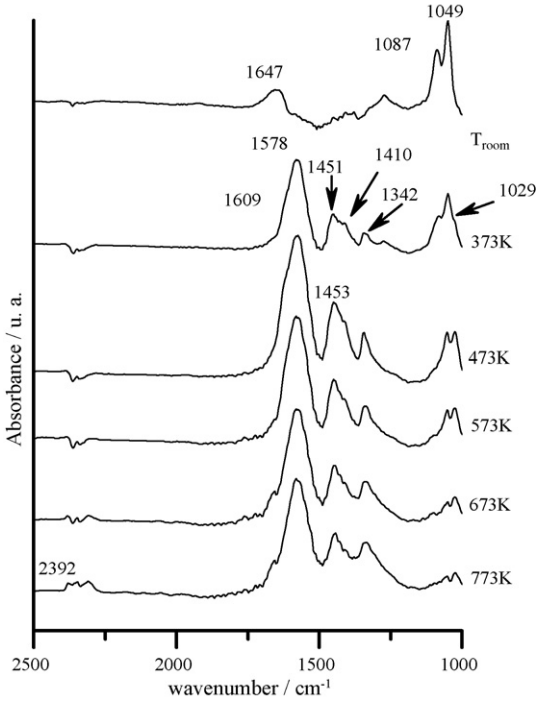

Fig. 8. Infrared spectra of the surface species formed by ethanol adsorption on Ru/Y_2O_3 catalyst at different temperatures.

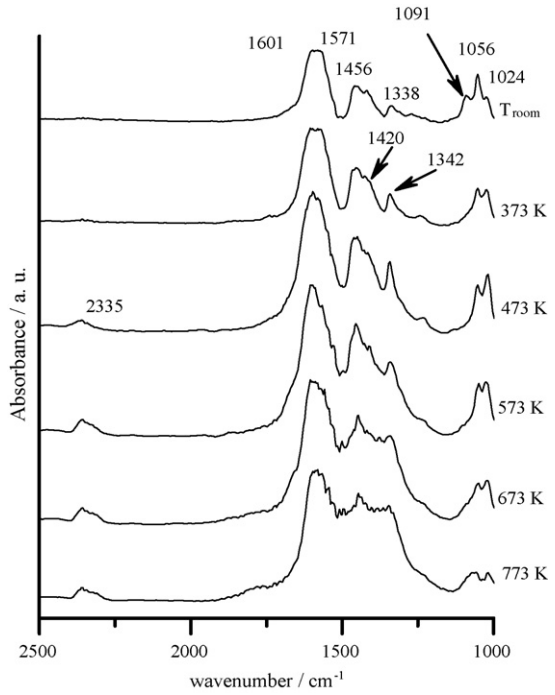

Fig. 9. Infrared spectra of the surface species formed by ethanol adsorption on Pd/Y_2O_3 catalyst at different temperatures.

were already detected even at room temperature in contrast with Y_2O_3 and Ru/Y_2O_3. It means that ethanol reactions on Pd differ from Ru.

At 373 K, the intensities of the bands corresponding to acetate and hydrogen carbonate species increased while the bands ascribed to ethoxy species disappeared.

When the temperature was increased to 473 K, the bands assigned to acetate and hydrogen carbonate species increased, as observed on Ru/Y_2O_3 catalyst. However, at this temperature, the IR spectrum of Pd/Y_2O_3 catalyst already presented the CO_2 bands (2300–2400 cm^{-1}), which were only detected at 773 K on Ru/Y_2O_3 catalyst. Contrary to the results observed for Ru/Y_2O_3 catalyst, the acetate and carbonate species almost completely disappeared on the Pd/Y_2O_3 catalyst upon heating to 773 K, which led to the CO_2 formation.

3.5. Reaction mechanism

The partial oxidation of ethanol over Pd/CeO_2, Pt/CeO_2 and Co/CeO_2 catalysts was previously studied in the literature [25]. The catalytic performance was explained based on the IR, TPD and Temperature-Programmed Surface Reaction (TPSR) experiments and a reaction mechanism was proposed. According to this mechanism, adsorption of ethanol on the support gives rise to ethoxy species. A fraction of the ethoxy species dehydrogenate, producing acetaldehyde, which readily reacts with oxygen from the support, producing acetate species. The extension of the oxidation reaction depends on the amount of oxygen from the support, whose reduction degree is a function of the metal and pretreatment conditions. By increasing the temperature, another fraction of the ethoxy species migrates to the metal particle and is decomposed, forming CH_4, H_2 and CO. Furthermore, the acetate species previously formed can be decomposed to CH_4, CO and/or oxidized to CO_2 via carbonate species [40–42].

In this work, from the results of DRIFTS and catalytic experiments up to 773 K, the reaction pathway proposed to partial oxidation of ethanol over Y_2O_3 support, Ru/Y_2O_3 catalyst and Pd/Y_2O_3 catalyst is exhibited in Fig. 10.

According to this mechanism, the ethanol adsorbs on Y_2O_3, producing ethoxy species. These species can be dehydrogenated and/or decomposed on metal sites, producing H_2, CO and CH_4. The intermediate dehydrogenated species may desorb as acetaldehyde, which can be dehydrogenated to acetyl species. Increasing the temperature, the acetyl species can react with gas phase oxygen to form acetate species, which can be decomposed to CH_4, CO and/or oxidized to CO_2 via carbonate species. At temperatures higher than 773 K, CH_4 reacts with water and CO_2 formed, producing H_2 and CO.

Some reaction pathways are favored depending on the presence of the metal and the nature of the metal.

The products distribution obtained on partial oxidation of ethanol suggested that the presence of the metal (Ru or Pd) favored the decomposition of ethoxy species, since the Y_2O_3 supported Ru and Pd catalysts presented a higher production of H_2, CO and CH_4 at 473–773 K.

The higher CH_4 and CO formation at 673 K (Fig. 4) on the Pd/Y_2O_3 catalyst suggests that the decomposition of ethoxy species is promoted on this catalyst. This is indirectly responsible for the lower acetaldehyde formation since a lower fraction of ethoxy species undergo dehydrogenation. Furthermore, the formation of acetate and carbonate species was promoted on the Pd-based catalyst. This also explains the lower production of acetaldehyde on this system. The higher CO_2 production at low temperature is probably due to the CO oxidation, which was formed by the decomposition of the dehydrogenated species. In fact, Pd-based catalysts are generally used on CO combustion reaction and can explain the large CO_2 production on the Pd/Y_2O_3 catalyst. The CH_4 and CO_2 presence at high temperature is assigned to the decomposition of acetate species via carbonate species. In fact, this evidence agrees with DRIFTS analysis, which showed a decrease in the intensities of both acetate and carbonate bands and the appearance of the bands corresponding to CO_2 with an increase in temperature.

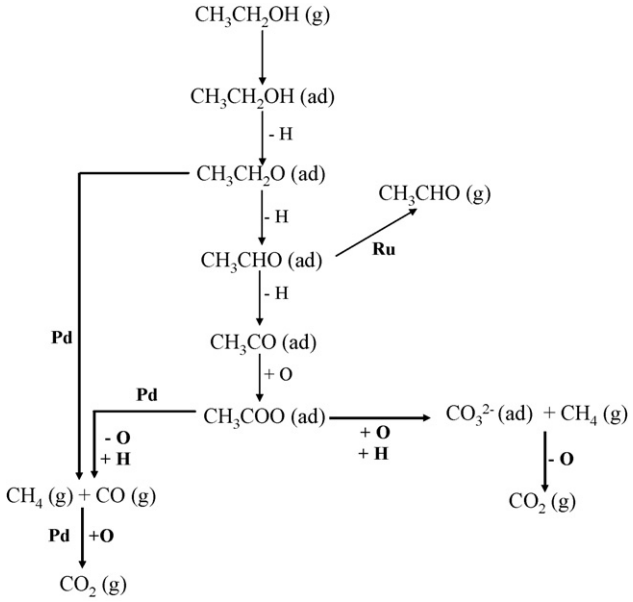

Fig. 10. Reaction pathway proposed to partial oxidation of ethanol over Ru/Y_2O_3 and Pd/Y_2O_3 catalysts.

On the other hand, the acetaldehyde desorption is promoted on Ru-based catalyst instead of its further dehydrogenation and production of acetate species. Actually, the acetate species remain quite stable at 773 K, which can explain the lower CO_2 and CH_4 formation on Ru/Y_2O_3 catalyst.

Above 873 K, the catalytic tests showed that ethanol was completely consumed and the only products are CH_4, CO, CO_2 and H_2. Increasing the reaction temperature decreased the methane selectivity while H_2 and CO formation increased simultaneously. These results suggest that the methane reacts with steam and CO_2 producing H_2 and CO. Ru/Y_2O_3 catalyst was more effective to this reaction than the Pd-based catalyst.

4. Conclusions

The product distribution obtained for partial oxidation of ethanol over Y_2O_3 supported catalysts was strongly affected by the metal nature. H_2 production and acetaldehyde formation

was higher on Ru-based catalyst. On the other hand, Pd/Y_2O_3 catalyst exhibited a higher formation of CO and methane. These results were explained by a reaction pathway determined by using DRIFTS experiments. The adsorption of ethanol gives rise to ethoxy species on both catalysts. These species can be decomposed, producing CH_4, H_2 and CO or dehydrogenated, forming acetaldehyde. The acetaldehyde species are dehydrogenated to acetyl species or desorbed. The acetyl species can be oxidized to acetate species or can be decomposed, forming CH_4, H_2 and CO. Furthermore, the acetate species previously formed can be decomposed to CH_4, CO and/or oxidized to CO_2 via carbonate species. On Pd/Y_2O_3 catalyst, the decomposition of ethoxy species was favored. This fact explained the higher CH_4 and CO formation and the lower acetaldehyde production at low temperature over Pd-based catalyst. On Ru/Y_2O_3 catalyst, the acetaldehyde desorption was promoted. Moreover, on Pd-based catalyst, the acetate and carbonate species formation were favored, which could also explain the lower production of acetaldehyde on this sample.

Acknowledgements

The authors wish to acknowledge the financial support of FINEP/CTPETRO/Petrobras (01.04.0891.00). L.O.O. Costa acknowledges the scholarship received from CAPES.

References

[1] M. Momirlan, T. Veziroglu, Renew. Sustain. Energy Rev. 3 (1999) 219.
[2] D. Das, T. Veziroglu, Int. J. Hydrogen Energy 26 (2001) 13.
[3] M.A. Pena, J.P. Gómez, J.L.G. Fierro, Appl. Catal. A 144 (1996) 7.
[4] D. Wang, S. Czernik, D. Mntané, M. Mann, E. Chornet, Ind. Eng. Chem. Res. 36 (1997) 1507.
[5] T. Rostrup-Nielsen, Catal. Today 106 (2005) 293.
[6] J.N. Armor, Catal. Lett. 101 (2005) 131.
[7] R. Ramachandran, R.K. Menon, Int. J. Hydrogen Energy 23 (1998) 593.
[8] S.A. Sherif, F. Barbir, T.N. Veziroglu, Electricity J. 18 (2005) 62.
[9] J.M. Ogden, T.G. Kreutz, M.M. Steinbugler, Fuel Cells Bull. 16 (2000) 5.
[10] J.R. Rostrup-Nielsen, Phys. Chem. Chem. Phys. 3 (2001) 283.
[11] S. Freni, N. Mondello, S. Cavallaro, G. Cacciola, V.N. Parmon, V.A. Sobyanin, React. Kinet. Catal. Lett. 71 (2000) 143.
[12] V.V. Galvita, G.L. Semin, V.D. Belyaev, V.A. Semikolenov, P. Tsiakaras, V.A. Sobyanin, Appl. Catal. A: Gen. 220 (2001) 123.
[13] A.N. Fatsikostas, D.I. Kondarides, X.E. Verykios, Chem. Commun. (2001) 851.
[14] S. Cavallaro, N. Mondello, S. Freni, J. Power Sources 102 (2001) 198.
[15] A.N. Fatsikostas, D.I. Kondarides, X.E. Verykios, Catal. Today 75 (2002) 145.
[16] J. Llorca, N. Homs, J. Sales, P.R. de la Piscina, J. Catal. 209 (2002) 306.
[17] M.A. Goula, S.K. Kontou, P.E. Tsiakaras, Appl. Catal. B: Environ. 49 (2004) 135.
[18] E.C. Wanat, K. Venkataraman, L.D. Schmidt, Appl. Catal. A.: Gen. 276 (2004) 155.
[19] J. Kugai, S. Velu, C. Song, Catal. Lett. 101 (2005) 255.
[20] S. Velu, N. Satoh, C.S. Gopinath, K. Suzuki, Catal. Lett. 82 (2002) 145.
[21] G.A. Deluga, J.R. Salge, L.D. Schmidt, X.E. Verykios, Science 303 (2004) 993.
[22] R.M. Navarroa, M.C. Álvarez-Galván, M. Cruz Sánchez-Sánchez, F. Rosab, J.L.G. Fierro, Appl. Catal. B.: Environ. 55 (2005) 229.
[23] V. Fierro, V. Klouz, O. Akdim, C. Mirodatos, Catal. Today 75 (2002) 141.
[24] L.V. Mattos, F.B. Noronha, J. Power Sources 152 (2005) 50.
[25] L.V. Mattos, F.B. Noronha, J. Power Sources 145 (2005) 10.
[26] L.V. Mattos, F.B. Noronha, J. Catal. 233 (2005) 453.
[27] J.R. Salge, G.A. Deluga, L.D. Schmidt, J. Catal. 235 (2005) 69.
[28] W. Wang, Z. Wang, Y. Ding, J. Xi, G. Lu, Catal. Lett. 81 (2002) 63.
[29] S. Cavallaro, V. Chiodo, A. Vita, S. Freni, J. Power Sources 123 (2003) 10.
[30] A.N. Fatsikostas, X.E. Verykios, J. Catal. 225 (2004) 439.
[31] M. Guil, N. Homs, J. Llorca, P.R. de la Piscina, J. Phys. Chem. B 109 (2005) 10813.
[32] A. Haryanto, S. Fernando, N. Murali, S. Adhikari, Energy Fuels 19 (2005) 2098.
[33] P.D. Vaidya, A.E. Rodrigues, Chem. Eng. J. 117 (2006) 39.
[34] V. Fierro, O. Akdim, H. Provendier, C. Mirodatos, J. Power Sources 145 (2005) 659.
[35] M. Mavrikakis, M.A. Barteau, J. Mol. Catal. 131 (1998) 135.
[36] J.P. Breen, R. Burch, H.M. Coleman, Appl. Catal. B 39 (2002) 65.
[37] M.S. Batista, R.K.S. Santos, E.M. Assaf, J.M. Assaf, E.A. Ticianelli, J. Power Sources 124 (2003) 99.
[38] J. Llorca, J.A. Dalmon, P.R. de la Pisicina, N. Homs, Appl. Catal. A 243 (2003) 261.
[39] H. Idriss, C. Diagne, J.P. Hindermann, A. Kiennermann, M.A. Barteau, J. Catal. 155 (1995) 219.
[40] A. Yee, S.J. Morrison, H. Idriss, J. Catal. 186 (1999) 279.
[41] A. Yee, S.J. Morrison, H. Idriss, J. Catal. 191 (2000) 30.
[42] A. Yee, S.J. Morrison, H. Idriss, Catal. Today 63 (2000) 327.
[43] C. Binet, M. Daturi, J.C. Lavalley, Catal. Today 50 (1999) 207.
[44] C. Binet, A. Jadi, J.C. Lavalley, J. Chim. Phys. 89 (1992) 1779.
[45] K.I. Gursahani, R. Alcalá, R.D. Cortright, J.A. Dumesic, Appl. Catal. 222 (2001) 369.
[46] M.A.S. Baldanza, L.F. de Mello, A. Vannice, F.B. Noronha, M. Schmal, J. Catal. 192 (2000) 64.
[47] L.F. de Mello, F.B. Noronha, M. Schmal, J. Catal. 220 (2003) 358.
[48] E.M. Cordi, J.L. Falconer, J. Catal. 162 (1996) 104.